

# Shale Wettability Characteristics via Air/Brines and Air/Oil Contact Angles and Influence of Controlling Factors: A Case Study of Lower Indus Basin, Pakistan

Darya Khan Bhutto, Abdul Majeed Shar,\* Ghazanfer Raza Abbasi, and Ubedullah Ansari



Cite This: *ACS Omega* 2023, 8, 688–701



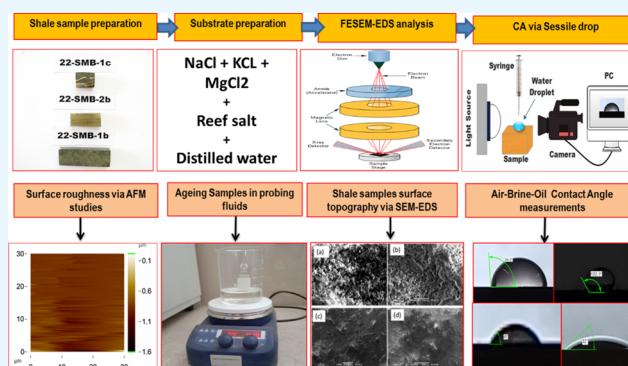
Read Online

ACCESS |

Metrics & More

Article Recommendations

**ABSTRACT:** Wettability is the fundamental parameter that influences the productivity of hydrocarbon reservoirs. The knowledge of this regarding shale formation is yet inadequate; thus, detailed analysis is essential for successful development of such reservoirs. The Early Cretaceous Sembar formations in the Lower Indus Basin, Pakistan, is considered as the key target for energy exploration; however, it exhibits large uncertainties due to the lack of data availability. Sembar shales hold significant hydrocarbon volumes rich in organic content; however, prior to this, no comprehensive research has been conducted to quantify the wetting behavior of these shales. Thus, precise information about the wetting behavior of Sembar shale formations is essential, as it is influenced by many factors. Therefore, in this study, we examined the wettability of Sembar shale samples by performing a suit of contact angle (CA) measurements. The CA measurements on shale samples were performed using different salt types (NaCl, KCl, MgCl<sub>2</sub>, and Reef Salt) and concentrations of 0.1 M and 0.5 M under ambient pressures and varying temperatures (25–50 °C). The CA was measured via air–brine and air–oil under prevailing pressure and temperature conditions. Subsequently, the sample morphology and surface topography were examined via field emission scanning electron microscopy and atomic force microscopy, respectively. The mineral compositions were obtained via X-ray diffraction studies. The results clearly show that the Sembar shale possesses a mixed wetting behavior. Under dry surfaces, they have large affinity to oil and deionized water in which the droplet spreads quickly on the sample surfaces. Conversely, the samples aged with *n*-decane and NaCl brines exhibited higher CAs than the untreated samples. Additionally, the CA measured by changing temperatures led to an increase for all brine droplets; the CA further increased as the concentrations of salts increased from 0.1 to 0.5 M. We then discussed the possible reasons for the discrepancy in CA values due to temperature changes and brine concentrations. Moreover, the CA was measured corresponding to the surface roughness from which it appears that it merely affects the wettability of these shale samples. However, the present study results lead to an improved understanding of the wettability of Sembar shale of the Lower Indus Basin in Pakistan.



## 1. INTRODUCTION

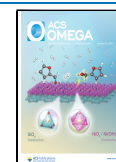
For the exploitation and development of efficient oil and gas reservoirs, wettability plays the most significant role and controls the fluid flow, as well as affects the productivity of the reservoirs.<sup>1–7</sup> It is commonly held that wettability is a physiochemical parameter that depends on the fluid–rock interactions, total organic content (TOC), interfacial tension, thermal maturity, mineral compositions, and surface roughness and rock physical properties.<sup>8–13</sup> Thus, the wettability of shales is affected by various parameters from the presence of organic matter, rock composition, to mineral–grain orientations. However, shales are not fully characterized in terms of their wettability characteristics. Thus, it is important to assess the characteristics of shale wettability for unconventional energy resources for successful exploitation and development.<sup>8,14</sup>

Thus, assessing the wettability characteristics is important as it mainly affects the rock and fracturing fluids, which are treatment fluids following unconventional fracturing operations for reservoir development.<sup>15</sup> Essentially, the shale formation is composed of a combination of various mineral constituents (e.g., clay, quartz, calcite, feldspars, and iron oxides) and organic compounds which are found in varying quantities within heterogeneous shale rocks.<sup>16–18</sup> However, the

Received: September 14, 2022

Accepted: December 21, 2022

Published: December 29, 2022



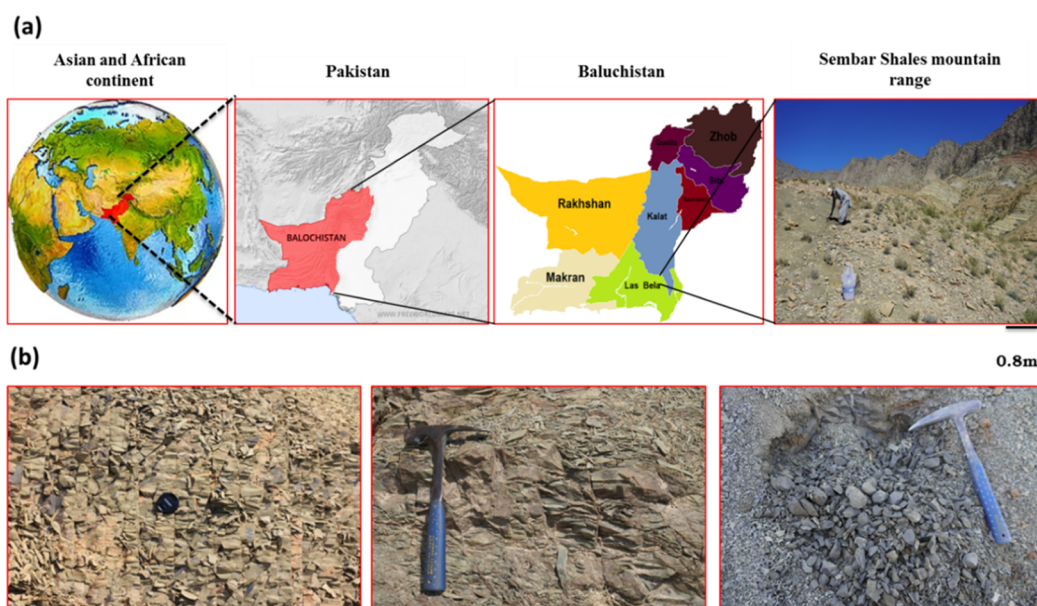


**Figure 1.** Geological map of Pakistan along with (a) outcrop view of the Sembar shale formation and (b) sample collection site in the Lower Indus Basin, Pakistan.

**Table 1.** List of Collected Samples, Their Localities, and Geographic Coordinates (UTM)

station no.	sample no.	coordinates	location	latitude	longitude
Winder city area, Balochistan	Sembar shale	N 25° 56.708, E 66° 56.477	Winder city area near the Pab mountain range approximately 650 m off to the Khurkhera-Kanjraj Road	25.80067	66.91412

wettability of the shale formation is very complex to understand, which in turn displays the different wetting tendencies from hydrophobic to hydrophilic and to mixed wettability.<sup>19–21</sup> In the literature, some published studies reported that the shales possess a hydrophilic behavior;<sup>22–24</sup> on the contrary, other studies have claimed that they are hydrophobic,<sup>21,25,26</sup> and some of them provided that they exhibit mixed wettability.<sup>27,28</sup> The reason for such differences in the wettability of shale rocks is the discrepancies in mineralogical composition and textural parameters,<sup>29</sup> complex pore distributions,<sup>20,30,31</sup> and the presence of organic matter in varying quantities.<sup>25,32,33</sup> Usually, the wettability of conventional reservoirs is obtained by any of the methods mentioned, such as (i) the contact angle (CA) method, (ii) the drainage and imbibition method, (iii) atomic force microscopy (AFM), and (iv) nuclear magnetic resonance and zeta potential.<sup>29,34–37</sup> However, the shale formation is extremely tight, exhibiting magnitude of orders lower permeability than the conventional reservoirs; thus, most of the pores are of micro- to nanometer sizes. Hence, in these ultra-low-permeability formations, most of the above-mentioned methods of wettability quantification are inconvenient except the CA method, which is more suitable. In addition, a complex pore network and extremely low-permeability and rock heterogeneities also limit the applications of methods other than CAs.<sup>4</sup> In addition, the rock surface roughness significantly influences the CA measurements. Previously, few studies have attempted to assess the wettability considering the rock surface roughness.<sup>38</sup> Theoretical models were developed to quantify the wettability of smooth and rough surfaces, that is, Young's equation, the Wenzel model, and the Cassie–Baxter equation. Young<sup>39</sup> studied the wetting tendency of the solid surface in environments of very regular surfaces. However, Wenzel<sup>40</sup>

and Cassie and Baxter<sup>41</sup> proposed that there may be air gaps on the surface topography of coarse solid surfaces; hence, the CA measured by considering uneven surfaces of samples under rough surfaces is significantly influenced by the wetting affinity.<sup>42</sup> On the contrary, other studies have proposed that surface roughness has a slight impact on the CA results of carbonate samples.<sup>3</sup> In addition, temperatures significantly affect the shale rock wettability. However, the pressures are considered to affect the wettability of rocks slightly.<sup>43</sup> However, the wettability experiments under pressure changes were not considered to be conducted due to their insignificant effects. Moreover, several studies have been carried out to understand the wetting behavior via laboratory attempts for shales.<sup>44–46</sup> However, none has yet reached in providing the unified conclusion. Thus, it is very challenging to reach unique conclusions regarding the shale rock wetting characteristics to various fluids.

Thus, this study has comprehensively investigated the air/brine/ and air–oil/rock system's wetting affinity of Sembar shale formations in the Lower Indus Basin, Pakistan, as a function of brine type, composition, temperature, and sample surface roughness. A wide range of salt solutions with different concentrations such as NaCl, KCl, MgCl<sub>2</sub>, Reef Salt, and deionized water were tested under varying conditions of temperature. Further, the CA of the Sembar shale samples was obtained considering different salt types and concentrations. Finally, an attempt was made to assess the impact by variations in the mineral compositions of shales and various other factors that are responsible for changes in the CA of these shales.

Geological Settings: Pakistan possesses the largest sedimentary basin covering the most underexplored unconventional potential of fossil fuels.<sup>13,47–49</sup> The Indus Basin of Pakistan is one of the significant sedimentary basins that



**Figure 2.** Illustration shows the (a) photograph of the shale sample hand specimen and (b) sample prepared for CA measurements.



**Figure 3.** Salt stock and brine solutions prepared by blending with a desired amount of salts in distilled water under different temperature conditions.

contains huge unexplored resources in its unconventional formations. The study area and sampling sites are shown in Figure 1a,b. The details of sampling points and their geographic locations along with their coordinates are provided in Table 1. The Sembar formation was observed from the base of the Pab range starting from 150 to 200 m-thick rocks of dolerite composition. The mountain peak at the Pab succession is encroached by Jurassic Limestone at the top and was followed by the Sembar shale formation with a thickness of around 25–30 m. The color of the Sembar shales found in the Indus Basin was observed as light greenish to gray. On the other hand, as we traveled along the Pab range rocks, the color change of the shale formation to dark black and dark gray was perceived. At this location, few samples of the Sembar shales were picked, and it was observed that these contained iron stains of yellowish orange color. Most of the Sembar shales in the Lower Indus Basin are of the age of the Lower Cretaceous.<sup>50,51</sup> The iron nodules within the Sembar formations were also seen to range from 12 to 15 cm. These iron nodules were mainly limnetic in color. The Sembar shale formation changed from shale to mudstone intervals, and these were associated with fine silty sand beds covered by the thick Goru formations. The gross thickness of the Sembar formation as observed was around 40–60 m. These were overlain by thin variable intervals of siltstone, marl, and shale and mudstone beds.

## 2. EXPERIMENTAL METHODOLOGY

**2.1. Sample Preparation and Aging Process.** Sembar shales from different locations of the Lower Indus Basin, Khurkhera-Kanraj Road, Balochistan, Pakistan, were obtained for analysis. Initially, the sample blocks were collected, which were tagged and appropriately labeled. Figure 2 shows the

hand specimen and rectangular samples for assessing their surface wetting tendencies. The samples were then cut with a high-precision cutter for desired sizes of (2 cm × 2 cm × 2 cm) for CA measurements. Subsequently, the samples were cleaned. The samples in Soxhlet for cleaning were left overnight to remove the residual impurities of the sample surfaces. The laboratory conditions of wettability measurement may differ from in situ reservoir conditions due to changes in temperature and pressure conditions. The temperature change significantly affects the wettability of rocks.<sup>15</sup> Thus, we measured the wettability of these shales by changing the temperature conditions. However, the pressures are considered to affect the wettability of rocks insignificantly.<sup>43</sup> Hence, the wettability experiments under higher pressures were not conducted by the present study.

The CA measurements were made by aging with fluids of different brine concentrations and oils; a stock of different salts is displayed in Figure 3. Initially, the CA was measured using distilled water, and the subsequent measurements were made by aging the samples with 10 wt % seawater brines at a room temperature of 25 °C and atmospheric pressure. Four different brines were prepared to soak the samples and measure the CAs, that is, distilled water, NaCl, KCl, and MgCl<sub>2</sub> brines, and Reef Salt (seawater compositions) was also selected to measure the brine CA. The compositional details of brines prepared for CA measurements are shown in Table 2. In addition, the shale formation CA was quantified under surface roughness experiments to compare the CA with rough surfaces. The surface roughness was obtained using the AFM model of ezAFM + c10.20.16.51 Nano Magnetics imaging instrument with the tapping mode.

**2.2. X-ray Diffraction Analysis.** For X-ray diffraction (XRD) analysis, we prepared the powder of shale samples;

**Table 2. Properties of Brines Used for CA Measurements**

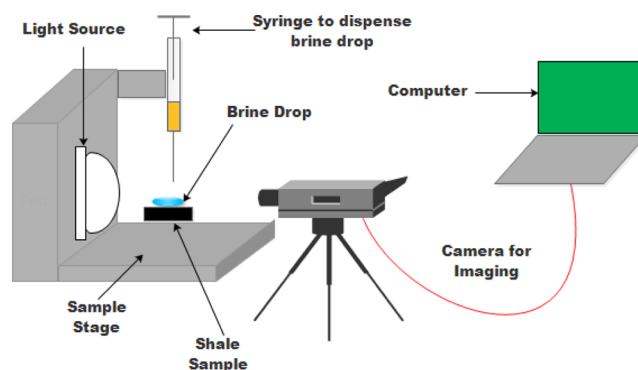
formation brine composition	pH (24 °C)	pH (40 °C)	density (g/cc)	TDS
NaCl	6.60–7.01	6.52–7.02	0.980–1.002	27,596
KCl	6.30–6.99	6.20–6.80	1.010–1.025	24,214
MgCl <sub>2</sub>	6.90–7.20	6.60–7.20	1.012–1.112	24,200

initially, the samples were cut in a rectangular shape by a precision knife cutter. These samples were very thin in thickness, which were ground to make a powder for quantitative analysis. The analysis was performed using a PANalytical X-ray diffractometer model number PW3040/60 X'Pert Pro, Amsterdam, The Netherlands. This setup was used to analyze the different phases in the Sembar shale samples. The X-ray diffractometer was run at room temperature at a current of 30 mA provided with a voltage of 40 kV, and scans were done with a step of 0.025 and CuK radiation.

**2.3. Scanning Electron Microscopy and Elemental Mapping.** We used field emission scanning electron microscopy and energy-dispersive spectroscopy (EDS) for surface topographic analysis and elemental mapping consequently. This instrument consists of secondary electrons, backscattered electrons, and an EDS electron detector for surface characterization and elemental identification. A secondary electron routine was adopted to analyze the surface topography, while heavy and light compounds of samples are detected via BSE. The elemental mapping of samples is usually obtained by the use of an EDS electron detector. For precise information of sample composition, the EDS analysis was aided with XRD quantifications.

**2.4. Surface Roughness of Samples via AFM.** To obtain smooth surfaces of the shale samples, the samples were polished using the 1000 mesh and 240 mesh sandpaper. For better visualization of surface topography changes of the Sembar shale formation, the samples were further polished using the alumina powder and silk cloth to remove all dirt and scrap. For surface topographic features, the experiments were performed via AFM. The AFM model of the ezAFM + c10.20.16.51 Nano Magnetics imaging instrument with the tapping mode was used to obtain the surface topographic images. The Sembar shale samples were cut into small cubic size with a knife cutter of sizes around 2.0–2.50 cm. However, the samples were prepared as per the desired size of the sample holder platen system. The samples were polished to make their surfaces smooth with fine paper of mesh size ranging from 400 to 5000. The samples of desired sizes of approximately 10 mm × 10 mm × 2 mm were prepared. It is to ensure that the aged sides of the samples must not be altered and ground because these surfaces were exposed for better visualization of surface roughness.

**2.5. CA Measurement Setup.** To investigate the surface wetting behavior of shale rocks, a widely used CA measurement method via drop analysis was used as displayed in Figures 4 and 5. The CA measurements were made after the preparation of sample chips of size ranging from 2 cm × 2 cm × 2 cm. The CA of flat shale sample chip surfaces was determined by viewing the probing fluid shape developed on the sample surface. The affinity to shale samples was analyzed by using different probing fluids. Initially, the NaCl, KCl, MgCl<sub>2</sub>, and Reef Salt solutions of two different concentrations were prepared. All the prepared brines were filled in a closed

**Figure 4.** Schematic illustration of experimental arrangement for CA measurements.

container and tightly closed to avoid evaporation of water to maintain the brine composition.

The experimental setup comprised light sources, syringes with different needles, a temperature-controlled bath (max temp. 150 °C), a digital camera for image recording, and a laptop for data processing as shown in Figure 4. The measurement of CA was made at ambient conditions initially. Then, a syringe filled with slightly more brines than the desired quantity and must be checked for tightness. For different brine compositions, different syringes were used as probing liquids. Around 50  $\mu$ L to 20 mL of probing liquids were prepared and placed in a cup as spare if required to be filled as desired. A piece of containment free cloth was used to remove excessive air bubbles or filths on the tip of the syringe needles. Later, we put the sample on the sample stage as shown in Figure 4. It is to ensure that there must not be any tilt on the surface that is holding the samples in either direction. After placing and fixing the shale samples on the sample stage then, a drop of brine was dispensed through the needle tip; subsequently, the position of the needle tip was lowered; thus, a drop of brine fell on sample surface. Then, we captured pictures via a digital camera. The CA precise measurements are very critical; hence, we repeated measurements three times to get the mean values. Thus, the process was repeated until the desired results are achieved. The experimental setup shows the needle position and corresponding camera for capturing the images. The images taken were further analyzed using ImageJ software (Figure 5).

### 3. RESULTS

**3.1. Total Organic Content.** TOC is the total organic carbon that is found to be present in a source rock and is represented as weight percent. Additionally, it indicates the total amount of organic matter that is present within the fine sedimentary shale rock formation, which shows rich content to generate the hydrocarbon potential. The TOC of the samples from Sembar shale gas was obtained using the Rock Eval equipment from Vinci Technologies, Nanterre, France. The TOC was experimentally determined by taking a small piece of the shale rock, which is ground to a fine powder. The results revealed that the Sembar shale samples exhibit 0.03–2.54 wt %, which shows that these samples have a reasonably good OM content.

**3.2. Characterization via XRD.** For the purpose of comparing the fluid wetting tendency, it is essential to know these shale compositions. Thus, we performed quantitative XRD analysis of these shales to assess the relative affinity of the compounds to probing fluids. The results of the XRD studies

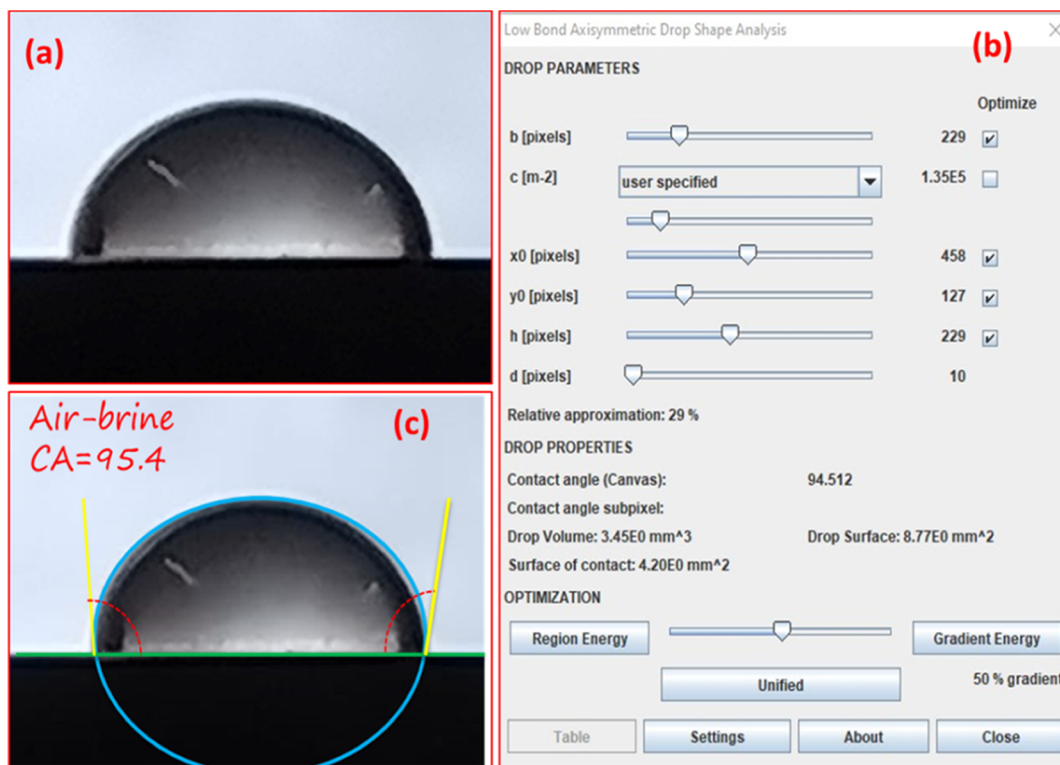


**Figure 5.** Illustration shows the (a) representative CA image, (b) ImageJ software window, and (c) CA determined via the drop shape analysis.

showed different mineral components and were predominantly composed of five main mineral compounds (Figure 6 and Table 3). The XRD analysis specifies the existence of different clay mineral types in all the samples and in variable quantities. These shales mainly consist of the silicon oxides ( $\text{SiO}_2$ ) with fragments of kaolinite, Fe-rich chlorite, mica silts, and illite-montmorillonite clays. In addition, illite-smectite types of clays were also detected along with traces of iron oxides and carbonates. The XRD studies show that illite is present in the Sembar shales varying from 6.48 to 41.2 wt %, kaolinite varies from 12.35 to 52.34%, and smectite is found to be present in these shales varying from 5.25 to 25.75 wt %. Chlorites found are in very small quantities. The first main compound of these shales was categorized as it possesses silicon oxides ( $\text{SiO}_2$ ). The second predominant compound was smectite and is called the montmorillonite clay. The third group compound name is illite-montmorillonite clay and is composed of aluminum, magnesium, and silicate hydroxide elements. The fourth one is the potassium iron magnesium aluminum silicate hydrate; this mineral is revealed to be the illite type of clay which is white in color. The subsequent compound detected through XRD studies is illite. The preceding smallest compound observed in the Sembar formation shale includes chlorite, potassium feldspars, iron, and titanium.

**3.3. Scanning Electron Microscopy and Energy-Dispersive X-ray Spectroscopy.** It is essential to identify the rock minerals for comparable affinity of minerals with probing fluids, that is, oil and brines. For this reason, we performed elemental analysis of our shale samples using SEM/EDS analysis. The elemental mapping of samples from EDS analysis obtained is shown in Figure 7. The SEM images taken shows the surface topography of these shales, and their corresponding elemental compositional variations were obtained via mineral mapping. We observed some dark spots

showing the organic matter within these samples. The bright spots on the SEM photomicrograph show that these shales also contain the pyrites. In some place in SEM photomicrographs, we observed dark spots which displayed iron oxides within these samples. Moreover, the XRD studies have aided in the recognition of quartz, chlorite, kaolinite, and other clay mineral types such as illite-montmorillonite as well as potassium feldspar clay minerals. The EDS elemental analysis also showed the presence of mica, which has a chemical composition of  $\text{K-Mg-Fe-AlSiO}_2\text{-H}_2\text{O}$ . The clay minerals are found to be present in all the studied samples of the Sembar shale formation under the SEM study.

**3.4. Atomic Force Microscopy.** The samples from Sembar shales for surface smoothness were analyzed via AFM, and the results obtained are displayed in Figure 8. AFM was performed on shale samples which were pretreated to examine the impact of surface roughness on wettability. The average surface roughness of the Sembar shale was determined via AFM (Flex-Axiom, Nano-surf through a C3000i model controller) experiments.<sup>52,53</sup> The results show that Sembar shale samples exhibit 6.57–356 nm, which in turn reflects that these samples possess a significantly smooth to rough surface. Hence, it is usually expected that the samples which shows a smoother surface establish higher CA than the samples with rough surfaces, in particular to quartz-dominated samples under hydrophobic conditions.<sup>13</sup> In this study, we noticed changes in CAs as the roughness of the sample changes. Further, the influence of roughness on the CA is discussed in the subsequent section.

**3.5. Contact Angle.** **3.5.1. CA of Air–Brine under NaCl, KCl,  $\text{MgCl}_2$ , and Reef Salt.** To study the brine composition impact and resulting changes in wettability, several small shale samples in a rectangular shape of varying sizes were first cut and then cleaned. This was performed via a trimming machine and

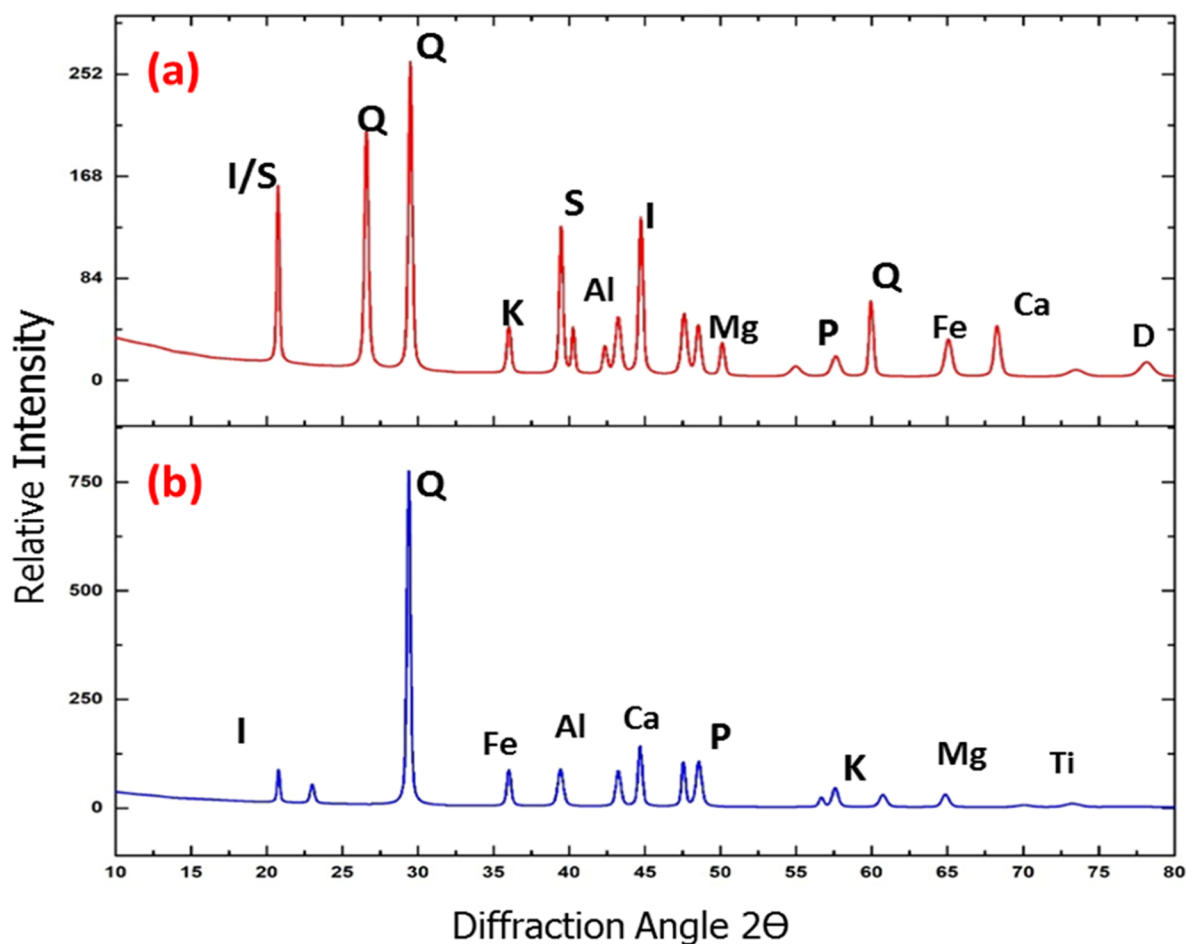


**Figure 6.** Illustration represents the XRD pattern from two different samples (a,b) which shows the mineralogy of shale from the Sembar Formation in the Lower Indus Basin, Pakistan. Explanation: (Q-quartz, I-illite, S-smectite Mg-magnesium, Al-aluminum, K-potassium-feldspars, P-pyrite, D-dolomite, Ca-calcite, S-siderite, and Fe-iron oxides).

**Table 3. Average Ranges of Mineral Content from Two of the Shale Samples (A and B) from the Sembar Formation**

mineral	sample A (wt %)	sample B (wt %)
quartz	52.57	45.12
kaolinite	12.4	14.3
chlorite	9.5	12.5
illite-montmorillonite	5.52	7.5
smectite	2.3	3.2
mica	5.4	5.41
calcite	5.3	5.43
iron oxides	2.3	2.35
dolomite	4.71	4.2
<b>total</b>	<b>100.0</b>	<b>100.0</b>

subsequently were gently polished to attain a reasonably smooth surface. After the preparation of the desired size and type of shale samples, these were then aged for a week in *n*-decane and NaCl concentrated salt solutions under room-temperature conditions. Then, the samples were horizontally positioned for CA measurement. For this reason, the digital camera was engaged to take the side images of brines and oil drops on shale sample surfaces. Initially, the CAs were measured via air–brines at a concentration of 0.10 M salt solutions (NaCl, KCl, MgCl<sub>2</sub>, and Reef Salt (seawater) under room temperature of 25 °C. Then, the CAs were measured by increasing the salt concentration to 0.5 M.

The CAs measured using different brine types and concentrations are shown in Figure 9 and Tables 4 and 5, respectively. The CA measurements carried out via different types of brine (NaCl, KCl, MgCl<sub>2</sub>, and Reef Salt (seawater) solutions at 0.1 M salt concentration are presented in Table 4. The results obtained using different brine droplets show that the MgCl<sub>2</sub> brine appeared to exhibit a larger CA after NaCl, followed by KCl, Reef Salt (seawater), and deionized water CAs. Further, it was noticed that the CAs consistently increased when the brine concentration was augmented. This increase in CAs noticed for almost all brine types when the temperatures were increased. The CA established due to NaCl brines was 94.4° (Table 4). On the other hand, it was found that the CA measured for deionized water on shale surfaces was 44.1° (Table 4). These reported results of CA measurement were recorded after water drop stabilization for 15 min at least. Although, the CAs measured immediately after dropping of probing fluids might not be applicable in assessing the wettability of shales. However, instantaneously measured CAs reflect higher CA values and poor wetting behavior for NaCl brines. Additionally, the temperature changes and vaporization of fluids, and probing fluid soaking, imbibition may change the shape of a drop.<sup>54</sup> From the present study results of Sembar shale CAs (Tables 4 and 5), it appears that MgCl<sub>2</sub> lead to the maximum value, followed by NaCl, KCl, and Reef Salt solutions at a given pressure and temperature, and these results

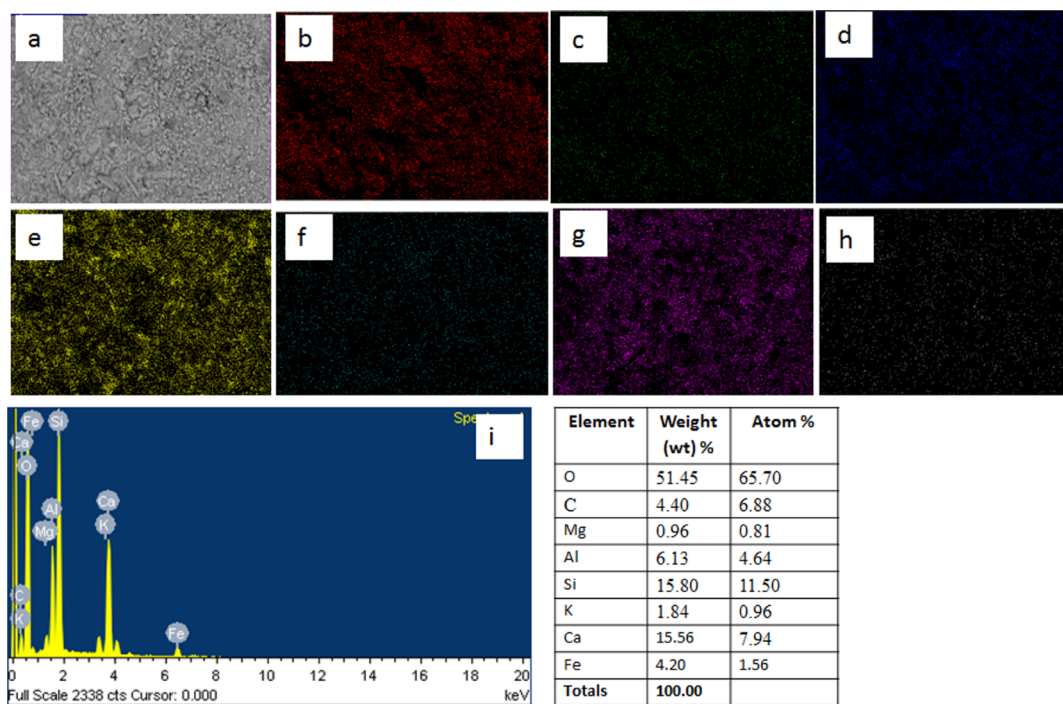


**Figure 7.** Photomicrograph from FESEM/EDS analysis of the Sembar shale shows the topography of 22-SMB-2a, which is predominantly composed of different elements. In this, (a) displays the SEM image and it is mainly composed of (b) O, (c) Mg, (d) Al, (e) Si, (f) K (g) Ca, and (h) Fe (iron) and (i) EDS elemental spectrum and the corresponding weights and atomic percentage are provided in table.

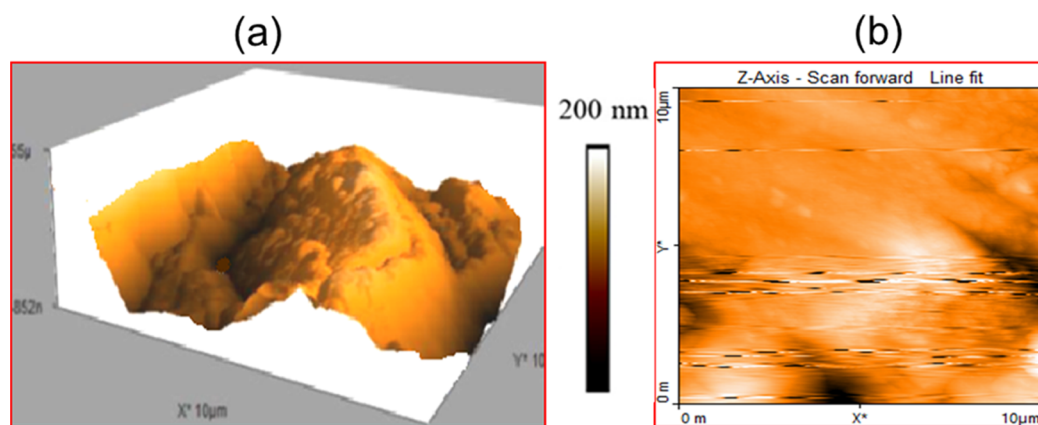


**Figure 8.** Surface morphology of the Sembar shale formation: (a) 3D and (b) 2D.

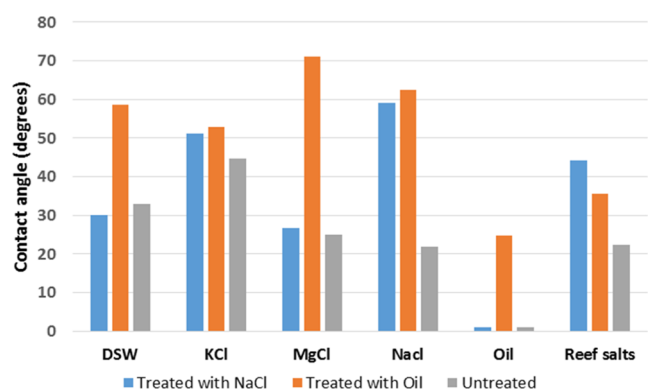


**Figure 9.** CAs measured at different ionic concentrations of DSW, NaCl, KCl, MgCl<sub>2</sub>, and Reef Salt (seawater) at 0.1 M salt concentration.

**Table 4.** CA Degrees Measured for all Cases in This Study Using Different Salt Types and Concentrations [KCl, NaCl, MgCl<sub>2</sub>, and Reef Salt (Seawater)]<sup>a</sup>

brine composition	CA (degrees)		
	(a) untreated samples	(b) treated samples with NaCl brine solution	(c) treated samples with <i>n</i> -decane
NaCl	94.4	59	62.5
KCl	44.7	51.10	52.9
MgCl <sub>2</sub>	26.6	71.2	32.0
Reef Salt (seawater)	25.1	44.7	52.8
deionized water	44.1	58.7	22.2
condensate air	0	90.4	65.4

<sup>a</sup>In the case of deionized water, the salt concentrations were zero.

**Table 5. CA Images of the Shale Sample Surfaces: (a) Untreated Samples, (b) Treated with Brines of NaCl Brine Solution, and (c) Treated with *n*-Decane**

Air-brine CA under salts concentration of (0.1 M)	(a) Untreated samples (CA)	(b) Treated samples with NaCl brine solution	(c) Treated samples with <i>n</i> -decane
KCl			
MgCl <sub>2</sub>			
NaCl			
Reef Salt (sea water)			
De-ionized water			

**Table 6. *n*-Decane CAs in Air Measured under Ambient Pressures and Temperatures**

System	Without treatment shale sample surface (CA)	Treated samples with NaCl brine solution (NaCl of 5g/L)	Treated Shale samples with <i>n</i> -decane
<i>n</i> -Decane -air	 Contact angle = 0.0°	 Contact angle = 90.4°	 Contact angle = 65.4°

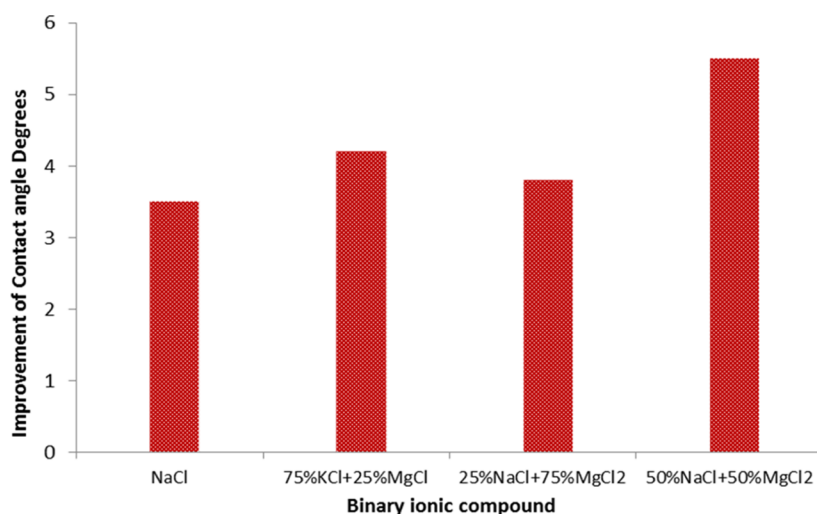


**Figure 10. CA increase results for binary ionic compound brine solutions (MgCl<sub>2</sub> + NaCl and KCl + MgCl<sub>2</sub>).**

are consistent with previously published studies.<sup>55–59</sup> Moreover, theoretically, it is apparent that an increase in ion concentration will lead to an increase in the CA; thus, the previous results also support this assertion and are consistent with the present study data. In addition, the various other published studies have also reported similar findings.<sup>21,60,61</sup>

**3.5.2. CA of Air–Oil on Shale Surface.** A drop of volume of *n*-decane was released from the syringe to fall on the Sembar shale surface for treated and untreated shale samples; subsequently, the air–oil CAs were measured. The results are presented in Table 6. The contact measured on the untreated shale sample surface via the *n*-decane droplet was zero, and the oil drop on the surface after falling spread

quickly. It was very difficult for a drop to stay on the sample surface, though it was vanishing right after falling on the sample surface. However, the CA for the sample treated with NaCl brines recorded instantaneously was 90.4°. Further after few minutes of time, the oil droplet started to spread rapidly over the shale sample surface, thus by complete wetting. It is important to express that if the drop did not display equilibrium attainment for air–brine drops, such measurement did not reflect reliable CAs. Thus, as mentioned above, when the oil droplet spreads completely over the shale sample surface, the resulting angle becomes 0°, which is considered as a stabilized CA. This similar behavior was perceived while taking the measurement for Sembar shale surfaces. The measurements were also repeated and the results for air–oil are shown in Table 6.

## 4. DISCUSSION

**4.1. Controlling Factors of CA.** The factors that significantly affect the shale wettability and the changes that occur due to modification in those include are the mineralogy, temperature and pressure conditions, TOC, mineral occurrences, surface roughness, and thermal maturity conditions. Thus, the effect of the aforementioned factors on shale wettability are subsequently analyzed and discussed.

**4.1.1. CA via Sample Treated with Binary Compound Salt Solutions [MgCl<sub>2</sub> + NaCl].** The CA measurements were carried out using binary compound salt solutions via an air–brine droplet on the shale sample surface under ambient condition of pressure and temperature as shown in Figure 10. The effect of binary solutions was assessed by preparing a mixture of salt solution via blending NaCl and MgCl<sub>2</sub> salt solutions. The results of CA obtained using the mixture of MgCl<sub>2</sub> + NaCl brine solution are shown in Figure 10. Initially, the ratio of binary salt solution was prepared by mixing 25% NaCl and 75% MgCl<sub>2</sub>, which shows that the increase in CA established with mixture is simply 2°. However, it is clear from the results that when we added MgCl<sub>2</sub> in NaCl at a concentration ratio of 50%:50%, the CA increased from 2 to 5.5°. However, the CA measured solely using MgCl<sub>2</sub> has appeared to be the highest CA compared to those of all other brine solutions. Conversely, adding 50% of MgCl<sub>2</sub> and 50% of NaCl has further increased the total CA. The purpose of performing such experiments under these conditions was to analyze the favorable concentration of brines which can improve the shale wettability as well as productivity of oil and gas. Therefore, it was found that addition MgCl<sub>2</sub> to NaCl brine solution could significantly alter the effect of the CA of Sembar shales only at a favorable salt concentration, such as 50% MgCl<sub>2</sub> + 50% NaCl. Furthermore, other studies have also provided that the blending of NaCl to MgCl<sub>2</sub> decreases the efficiency of MgCl<sub>2</sub> if it is used for EOR as a modified brine solution. Thus, this implies that elimination of NaCl also led to an adverse effect in EOR experiments reported in published studies.

**4.1.2. Effect of Temperature on CA.** CA measurements were done under varying temperature conditions in order to study the effects on the wettability of shale formations due to changes in temperatures. The pressure effects on CA are insignificant; hence, it was decided not to investigate the effects of pressure on CA during the analysis of the present study. Thus, the CA measurements were carried out by changing the temperature, and brine concentrations and salt types are presented in Table 7 and Figure 11a,b, respectively. An

**Table 7. CA in Degrees Measured for All Cases Under Varying Conditions of Salt Types and Concentrations at Different Temperatures**

brine compositions	temperature °C			
	25	30	35	45
NaCl (0.1 M)	94.5	96.2	98.0	102
NaCl (0.5 M)	96.8	98.6	102.5	108.4
KCl (0.1 M)	51.1	52.4	54.4	56.0
KCl (0.5 M)	52.3	54.2	56.4	60.5
MgCl <sub>2</sub> (0.1 M)	71.2	72.4	74.2	77.5
MgCl <sub>2</sub> (0.5 M)	72.6	73.4	75.5	79.2
Reef Salt (seawater) (0.1 M)	44.7	46.2	48.2	50.5
Reef Salt (seawater) (0.5 M)	46.5	48.2	51.4	55.3

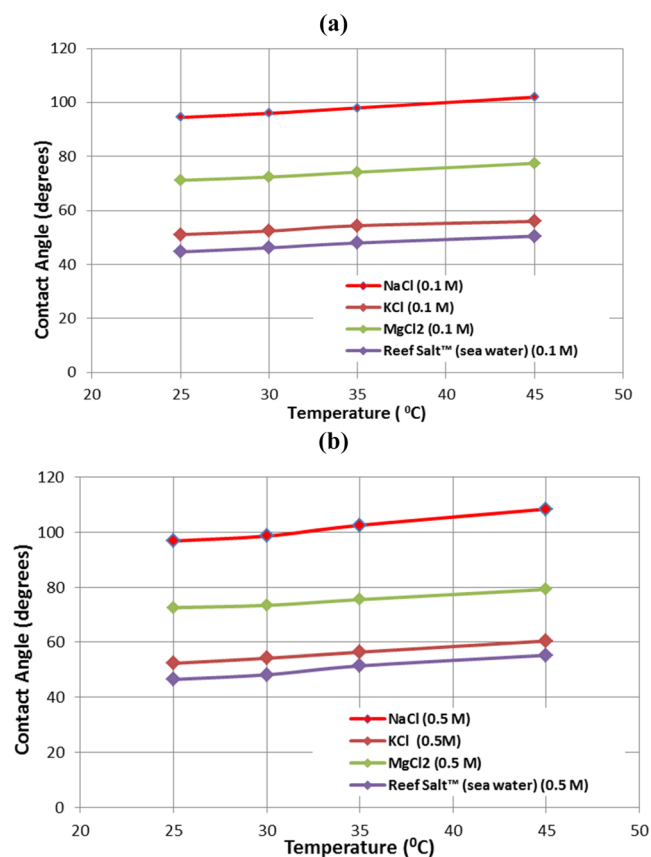


**Figure 11.** CAs measured (a) at 0.1 M salt concentration and (b) at 0.5 M salt concentration (NaCl, KCl, MgCl<sub>2</sub>, and Reef Salt solutions) as a function of salt type and varying temperatures.

increase in temperature from 25 to 50 °C led to a gradual rise in the CAs for all salt types from 0.1 and 0.5 M salt concentrations at prevailing conditions of pressure and temperature (Figure 11a,b). The extent of increase in CAs due to the increase in temperatures was higher at higher concentrations. For example, the CA increased by a maximum of 2° at 0.1 for most of the salt solutions at a temperature increase from 25 to 50 °C, whereas the change occurred in a CA of 0.5 M MgCl<sub>2</sub> brine due to the increase in temperature from 72.6 to 79.2° was significant than the lower concentration of 0.1 M under the same conditions of temperature increase. There is a contradiction in published studies regarding temperature changes and their influence on CAs. Few studies have reported that by the increase in temperature, the CA

measured increases,<sup>62–65</sup> as is the case of the present study; other studies have reported in contradiction, which provides that the CA decreases by the increase in temperature.<sup>58,66,67</sup> Thus, the effects of temperature on CA is ambiguous due to several parameters such as density differences, dielectric constants, interfacial tensions, fluid phases, and sample mineral compositions.

Many researchers have reported similar changes in CA behavior due to temperature changes. For example, Arif et al.<sup>3</sup> have reported that the increase in temperature decreases the CA values of the samples. In addition, the CA changes for coal resulting from CO<sub>2</sub> adsorption on coal surface were reported due to temperature increase.<sup>68</sup> Furthermore, other studies have also reported that the change in CA occurs by the increase of temperature for carbonate samples.<sup>69</sup> They found that the absolute value of crude oil/brine CA for carbonate increased from 72 to 77° at a temperature of 110 °C, which shows that a slight change in CA occurs for carbonate rocks. Similarly, in our study, we observed minor changes in CA values for shale samples due to changes in temperature from 25 to 50 °C. The slight reduction in the measured values of CA may be the result of droplet viscosity change due to temperature increase.

**4.2. Influence of Mineralogy on Shale Wettability.** The mineralogy of shale has significant influence in finding the wetting characteristics of surface rocks; thus, the shale formation surface is considerably crucial in determining their wettability. The shale formation exhibits various minerals in different proportions such as calcite, quartz, mica, chlorite kaolinite, and other clay mineral types such as illite-smectite and potassium feldspars. Therefore, the wettability is significantly affected by the mineral that is in dominance. In addition, it is reported that the TOC significantly affects the rock wettability as well as the interfacial tension.<sup>70</sup> For instance, Pan et al. 2020b describes the changes in interfacial tensions and wettability to shale A to shale B and C via their mineralogy.<sup>71</sup> Here, the sample that contains higher calcite content exhibits more hydrophobicity than others. Similarly, if the samples exhibit a higher amount of clay and mica minerals in shale B than shale type C, this led to more changes in  $\gamma$  rock–fluid interfacial changes in shale type B. In the present study, we analyzed the effects such as pressure, temperature, shale-TOC, and mineralogy on Sembar shale CA and wettability. However, attempts have been made to investigate the Sembar shale formations by considering realistic reservoir and geological environments. However, this may not cover all the actual conditions of reservoirs. For instance, the shale rocks earlier were treated as cap rocks; these may exhibit different mineralogy and wetting tendencies to different fluids affecting the reservoir adversely.

In this study, the wettability of untreated sample surfaces was measured and compared with that of the samples which were treated with brines and *n*-decane. The result obtained on the wettability of the Sembar shale samples established a dramatic change from complete water wetness to oil wettability. Therefore, the shale samples' aging for small time span altered their wetting tendencies from wetting to non-wetting conditions. Thus, for favorable treatment to shale reservoirs, accurate estimates of mineralogy are essential for wettability characteristics. Apart from mineralogy, the rock wettability is affected by brine salinity and concentrations, which may be in some situation is high enough. Moreover, the ion types also significantly affect the rock wettability as ions can be monovalent as Na<sup>+</sup>, K<sup>+</sup>, and Cl and divalent as these

factors affect the wettability considerably.<sup>72</sup> This study has simply analyzed the wettability of shale formations considering the effects of salt types, brine concentrations, TOC, mineralogy, and temperatures. However, the effects of ion types and valence could be further assessed. Therefore, the effects of salinity and type of ions will help in characterizing the shale formations.

**4.3. Influence of TOC on Shale Wettability.** The influence of the presence of organic matter on shale formation wettability to shale cap rock is extensively studied and is reported in the public domain. The wettability characteristics of shale cap rocks are significantly affected by the existence of organic matter into subsurface reservoirs.<sup>73–75</sup> The organic matter existence is unavoidable in the reservoir rock; thus, it is essential to assess the effects of organic matter on shale wettability. For example, the reported TOC data available in the public domain for Sembar shale formation ranges from 0.50 to 9.48 wt % (Ahmad et al. 2013 and Khalid et al. 2019), which shows that the Sembar shale exhibits poor to good OM maturity. Similarly, a present study finding also reveals that the Sembar shale possesses 0.03–2.54 wt %, which shows that this has good OM content.

The total organic matter and air–brine CA obtained are summarized in Figure 12. From the results, it is observed that

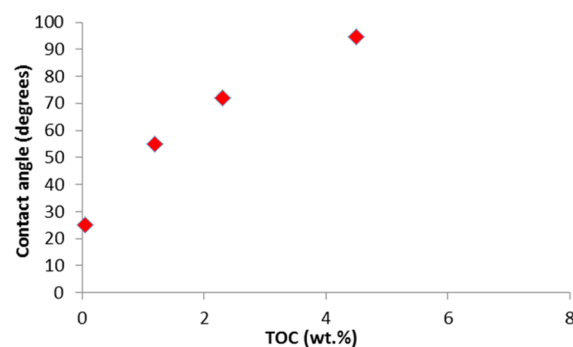


**Figure 12.** Influence of TOC on shale CAs.

with the increase in TOC, the CA is increased; for instance, at TOC increased from 0.05 to 2.54 wt %, the CA increases from 25 to 94.5°. This is ascertained by the results of other published studies reported as in Pan et al. 2021, in which it is mentioned that the rock surface hydrophobicity increase is due to the presence of organic matter.<sup>74</sup> On the other hand, the wetting behavior of shales in the case of shale gas presence shows reduction in wetting tendencies on shale sample surfaces with TOC as reported by other authors.<sup>13,74</sup> For instance, the results presented by Ali et al. 2022 show that  $\gamma$  shale–gas reduced from 103.26 to 86.85 mN/m, whereas the TOC was increasing from 0.08 to 14 wt %.<sup>13</sup> Other studies have also ascertained the phenomena and established that the TOC increases subsequently the hydrophobicity; thus, less energy is required for gas molecules to spread on the rock surface.<sup>76</sup> This implies that TOC is also an essential parameter that influences the shale formation wettability.

**4.4. Effect of Surface Roughness on Wettability in an Air/Brine/Water System.** The surface roughness significantly affects the dynamic wetting behavior of any of the material, and it can change the surface hydrophobicity. The surface roughness parameters (Ra) of the Sembar shale formation were acquired by processing the AFM data, and the results are displayed in Section 3.4, Figure 8, as 2D and 3D three-

dimensional images. The roughness (Ra) values were ranging from 6.57 to 356 nm with an average value of 253 nm (Table 8). The sample surface roughness values corresponding to the

**Table 8.** CA ( $\theta_{(a-brine)}$ ) Measured Using NaCl, KCl, MgCl<sub>2</sub>, and Reef Salt Solutions at 0.1 M Salt Concentration

sample ID	roughness (nm)	CA $\theta_{(a-brine)}$ NaCl	CA $\theta_{(a-brine)}$ KCl	CA $\theta_{(a-brine)}$ MgCl <sub>2</sub>	CA $\theta_{(a-brine)}$ Reef Salt	CA $\theta_{(a-water)}$ DI water
Sembar shale sample	253	95.6	52.4	72.4	45.2	25.5

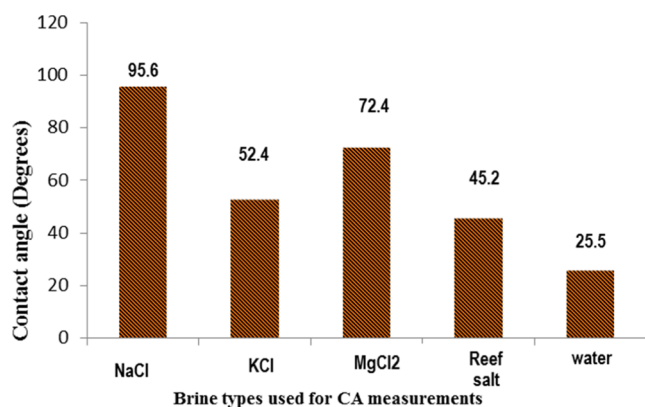


**Figure 13.** CAs measured via different brine types (NaCl, KCl, MgCl<sub>2</sub>, and Reef Salt solutions) at 0.1 M salt concentration under a roughness of 253 nm.

CA measured are illustrated in Figure 13. This yields that the Sembar shales are highly heterogeneous, exhibiting major surface irregularities; none of the sample has furnished smoother surface. This was consistent with the SEM images, which also displayed similar phenomena. The CA measurements were made using different brine types (NaCl, KCl, MgCl<sub>2</sub>, and Reef Salt solutions) at 0.1 M salt concentration and are provided in Table 8 ranging from 72.4 for MgCl<sub>2</sub>, which is the highest, followed by NaCl, KCl, and Reef Salt solutions under ambient temperature and pressure conditions. The lowest CA was established on deionized water. This implies that the lower the sample surface roughness, the smaller will be the impact on the wetting behavior as well as the CA will not be significantly affected.<sup>74</sup> It is noteworthy that the brine CA on the calcite sample in the existence of CO<sub>2</sub> reduced significantly from 85 to 75° due to the changes in sample surface roughness from 7.5 to 140 nm.<sup>74</sup> However, many other studies have also reported that the surface roughness significantly affects the CA of the samples. For example, in Papp and Csiha,<sup>77</sup> it is reported that there is a significant impact of surface roughness on the CA of various wood species. Hence, this requires careful investigation of measurements of shale sample wettability under realistic environments.

## 5. CONCLUSIONS

This paper has investigated the wettability of the Sembar shale formations in the Lower Indus Basin in Pakistan via CA measurements. For this purpose, the effects of different salt

types (NaCl, KCl, MgCl<sub>2</sub>, and Reef Salt) at concentrations (0.1 and 0.5 M) under ambient pressures and varying temperatures (25–50 °C) were studied. In addition, the CAs of oil as *n*-decane on the surface of the shale sample in air were also determined as a function of temperature and pressure. Thus, the factors influencing the wettability of shales were examined using the different salt type (NaCl, KCl, MgCl<sub>2</sub>, and Reef Salt) concentrations under varying temperature conditions, and the conclusions drawn are listed below.

1. The present study results provided that the brine CA measured for bivalent ions is higher than those measured using monovalent ion solutions. Subsequently, the CA measured using oil and brines of different concentrations have also shown an upward increase with an increase in prevailing conditions of temperatures, which in turn increases further if an ionic concentration of salt solution increases.
2. The CA measured via *n*-decane showed strong wetting affinity on untreated dry sample surfaces.
3. It was observed from the results that in most shale samples, the organic matter was absent. Thus, low organic matter maturity is the main factor for the Sembar shale formation with more hydrophilic rather than hydrophobic behavior.
4. The air–brine droplet ( $\theta_{a-b}$ ) binary compound salt solutions' (25% NaCl and 75% MgCl<sub>2</sub>) CA measured under ambient conditions of pressure and temperatures showed the increase in CA.
5. It was observed that the shale sample mineral composition and the characteristics of the surface roughness and an aqueous media, organic content deposits on the surface, and prevailing conditions of temperature and pressure all affect the wettability. The oil tends to spread quickly on shale sample surface and has more affinity compared to other minerals such as carbonate and siliceous minerals. Moreover, in the case of lower salt concentrations, the shale samples become more hydrophilic.

## AUTHOR INFORMATION

### Corresponding Author

Abdul Majeed Shar – Petroleum Engineering Department, NED University of Engineering and Technology, Karachi 75270, Pakistan; [orcid.org/0000-0003-4735-1660](https://orcid.org/0000-0003-4735-1660); Email: [majeed@neduet.edu.pk](mailto:majeed@neduet.edu.pk)

### Authors

Darya Khan Bhutto – Institute of Petroleum and Natural Gas Engineering, Mehran University of Engineering and Technology, Jamshoro, Sindh 76062, Pakistan; Department of Petroleum and Gas Engineering, Dawood University of Engineering and Technology, Karachi 74800, Pakistan  
Ghazanfer Raza Abbasi – School of Engineering, Edith Cowan University, Joondalup, Western Australia 6027, Australia; [orcid.org/0000-0001-8021-513X](https://orcid.org/0000-0001-8021-513X)

Ubedullah Ansari – Institute of Petroleum and Natural Gas Engineering, Mehran University of Engineering and Technology, Jamshoro, Sindh 76062, Pakistan

Complete contact information is available at: <https://pubs.acs.org/10.1021/acsomega.2c05960>

## Notes

The authors declare no competing financial interest.

## ACKNOWLEDGMENTS

The authors are highly grateful to the Asad Ali Narejo Geological Survey of Pakistan for assistance in doing field work. Professor Dr. Muhammad Hassan Agheem Centre for Pure & Applied Geology is greatly appreciated for his support in analyzing the XRD data. The authors are also indebted to Eng. Muhammad Ali Shar Baloch Researcher in King Abdullah Institute for Nanotechnology at the King Saud University, Riyadh Saudi Arabia, for FESEM.

## REFERENCES

- (1) Basu, S.; Sharma, M. M. Investigating the role of crude-oil components on wettability alteration using atomic force microscopy. *SPE J.* **1999**, *4*, 235–241.
- (2) Al-Anssari, S.; Arif, M.; Wang, S.; Barifcani, A.; Lebedev, M.; Iglauer, S. Wettability of nanofluid-modified oil-wet calcite at reservoir conditions. *Fuel* **2018**, *211*, 405–414.
- (3) Arif, M.; Abu-Khamsin, S. A.; Iglauer, S. Wettability of rock/CO<sub>2</sub>/brine and rock/oil/CO<sub>2</sub>-enriched-brine systems: Critical parametric analysis and future outlook. *Adv. Colloid Interface Sci.* **2019**, *268*, 91–113.
- (4) Yang, J.; Gu, C.; Chen, W.; Yuan, Y.; Wang, T.; Sun, J. Experimental Study of the Wettability Characteristic of Thermally Treated Shale. *ACS Omega* **2020**, *5*, 25891–25898.
- (5) Ali, M.; Jha, N. K.; Al-Yaseri, A.; Zhang, Y.; Iglauer, S.; Sarmadivaleh, M. Hydrogen wettability of quartz substrates exposed to organic acids; Implications for hydrogen geo-storage in sandstone reservoirs. *J. Petrol. Sci. Eng.* **2021**, *207*, 109081.
- (6) Iglauer, S.; Ali, M.; Keshavarz, A. Hydrogen wettability of sandstone reservoirs: implications for hydrogen geo-storage. *Geophys. Res. Lett.* **2021**, *48*, No. e2020GL090814.
- (7) Xue, H.; Dong, Z.; Tian, S.; Lu, S.; An, C.; Zhou, Y.; Li, B.; Xin, X. Characteristics of shale wettability by contact angle and its influencing factors: A case study in Songliao. *Front. Earth Sci.* **2021**, *9*, 736938.
- (8) Alvarez, J.; Schechter, D. Application of wettability alteration in the exploitation of unconventional liquid resources. *Petrol. Explor. Dev.* **2016**, *43*, 832–840.
- (9) Hatiboglu, C. U.; Babadagli, T. Experimental and visual analysis of co-and counter-current spontaneous imbibition for different viscosity ratios, interfacial tensions, and wettabilities. *J. Petrol. Sci. Eng.* **2010**, *70*, 214–228.
- (10) Buckley, J.; Takamura, K.; Morrow, N. Influence of electrical surface charges on the wetting properties of crude oils. *SPE Reservoir Eng.* **1989**, *4*, 332–340.
- (11) Anderson, W. G. Wettability literature survey-part 3: the effects of wettability on the electrical properties of porous media. *J. Petrol. Technol.* **1986**, *38*, 1371–1378.
- (12) Ali, M.; Aftab, A.; Arain, Z.-U.-A.; Al-Yaseri, A.; Roshan, H.; Saeedi, A.; Iglauer, S.; Sarmadivaleh, M. Influence of organic acid concentration on wettability alteration of cap-rock: implications for CO<sub>2</sub> trapping/storage. *ACS Appl. Mater. Interfaces* **2020**, *12*, 39850–39858.
- (13) Ali, M.; Pan, B.; Yekeen, N.; Al-Anssari, S.; Al-Anazi, A.; Keshavarz, A.; Iglauer, S.; Hoteit, H. Assessment of wettability and rock-fluid interfacial tension of caprock: Implications for hydrogen and carbon dioxide geo-storage. *Int. J. Hydrogen Energy* **2022**, *47*, 14104–14120.
- (14) Zhao, B.; MacMinn, C. W.; Juanes, R. Wettability control on multiphase flow in patterned microfluidics. *Proc. Natl. Acad. Sci.* **2016**, *113*, 10251–10256.
- (15) Habibi, A.; Binazadeh, M.; Dehghanpour, H.; Bryan, D.; Uswak, G. Advances in understanding wettability of tight oil

formations. *SPE Annual Technical Conference and Exhibition: OnePetro*, 2015.

(16) Loucks, R. G.; Reed, R. M.; Ruppel, S. C.; Hammes, U. Spectrum of pore types and networks in mudrocks and a descriptive classification for matrix-related mudrock pores. *AAPG Bull.* **2012**, *96*, 1071–1098.

(17) Curtis, M. E. Structural characterization of gas shales on the micro- and nano-scales. *Canadian Unconventional Resources and International Petroleum Conference; OnePetro*, 2010.

(18) Shar, A. M.; Ali, M.; Bhutto, D. K.; Alanazi, A.; Akhondzadeh, H.; Keshavarz, A.; Iglauer, S.; Hoteit, H. Cryogenic Liquid Nitrogen Fracking Effects on Petro-Physical and Morphological Characteristics of the Sembar Shale Gas Formation in the Lower Indus Basin, Pakistan. *Energy Fuels* **2022**, *36*, 13743.

(19) Alhammadi, A. M.; AlRatrou, A.; Singh, K.; Bijeljic, B.; Blunt, M. J. In situ characterization of mixed-wettability in a reservoir rock at subsurface conditions. *Sci. Rep.* **2017**, *7*, 10753.

(20) Dehghanpour, H.; Zubair, H.; Chhabra, A.; Ullah, A. Liquid intake of organic shales. *Energy Fuels* **2012**, *26*, 5750–5758.

(21) Borysenko, A.; Clennell, B.; Sedev, R.; Burgar, I.; Ralston, J.; Raven, M.; Dewhurst, D.; Liu, K. Experimental investigations of the wettability of clays and shales. *J. Geophys. Res. Solid Earth* **2009**, *114*, B07202.

(22) Roychaudhuri, B.; Tsotsis, T. T.; Jessen, K. An experimental investigation of spontaneous imbibition in gas shales. *J. Petrol. Sci. Eng.* **2013**, *111*, 87–97.

(23) Morsy, S.; Gomma, A.; Hughes, B.; Sheng, J. Improvement of Mancos Shale oil recovery by wettability alteration and mineral dissolution. *19th SPE Improved Oil Recovery Symposium, IOR 2014; Society of Petroleum Engineers (SPE)*, 2014; pp 73–82.

(24) Pan, B.; Li, Y.; Wang, H.; Jones, F.; Iglauer, S. CO<sub>2</sub> and CH<sub>4</sub> wettabilities of organic-rich shale. *Energy Fuels* **2018**, *32*, 1914–1922.

(25) Lan, Q.; Xu, M.; Binazadeh, M.; Dehghanpour, H.; Wood, J. M. A comparative investigation of shale wettability: The significance of pore connectivity. *J. Nat. Gas Sci. Eng.* **2015**, *27*, 1174–1188.

(26) Yassin, M. R.; Begum, M.; Dehghanpour, H. Source rock wettability: A Duvernay case study. *SPE/AAPG/SEG Unconventional Resources Technology Conference: OnePetro*, 2016.

(27) Blunt, M. J. *Multiphase Flow in Permeable Media: A Pore-Scale Perspective*; Cambridge University Press, 2017.

(28) Yang, R.; Hu, Q.; He, S.; Hao, F.; Guo, X.; Yi, J.; He, X. Pore structure, wettability and tracer migration in four leading shale formations in the Middle Yangtze Platform, China. *Mar. Petrol. Geol.* **2018**, *89*, 415–427.

(29) Siddiqui, M. A. Q.; Ali, S.; Fei, H.; Roshan, H. Current understanding of shale wettability: A review on contact angle measurements. *Earth-Sci. Rev.* **2018**, *181*, 1–11.

(30) Dehghanpour, H.; Lan, Q.; Saeed, Y.; Fei, H.; Qi, Z. Spontaneous imbibition of brine and oil in gas shales: Effect of water adsorption and resulting microfractures. *Energy Fuels* **2013**, *27*, 3039–3049.

(31) Roshan, H.; Oeser, M. A non-isothermal constitutive model for chemically active elastoplastic rocks. *Rock Mech. Rock Eng.* **2012**, *45*, 361–374.

(32) Liang, L.; Luo, D.; Liu, X.; Xiong, J. Experimental study on the wettability and adsorption characteristics of Longmaxi Formation shale in the Sichuan Basin, China. *J. Nat. Gas Sci. Eng.* **2016**, *33*, 1107–1118.

(33) Liang, L.; Xiong, J.; Liu, X. Experimental study on crack propagation in shale formations considering hydration and wettability. *J. Nat. Gas Sci. Eng.* **2015**, *23*, 492–499.

(34) Kumar, K.; Dao, E.; Mohanty, K. AFM study of mineral wettability with reservoir oils. *J. Colloid Interface Sci.* **2005**, *289*, 206–217.

(35) Hoxha, B.; Sullivan, G.; Van Oort, E.; Daigle, H.; Schindler, C. Determining the zeta potential of intact shales via electrophoresis. *SPE Europec featured at 78th EAGE Conference and Exhibition: OnePetro*, 2016.

- (36) Chen, J.; Hirasaki, G.; Flaum, M. NMR wettability indices: Effect of OBM on wettability and NMR responses. *J. Petrol. Sci. Eng.* **2006**, *52*, 161–171.
- (37) Li, C.; Singh, H.; Cai, J. Spontaneous imbibition in shale: A review of recent advances. *Capillarity* **2019**, *2*, 17–32.
- (38) Li, P.; Zhang, J.; Rezaee, R.; Dang, W.; Li, X.; Fauziah, C. A.; Nie, H.; Tang, X. Effects of swelling-clay and surface roughness on the wettability of transitional shale. *J. Petrol. Sci. Eng.* **2021**, *196*, 108007.
- (39) Young, T., III. An essay on the cohesion of fluids. *Phil. Trans. Roy. Soc. Lond.* **1805**, *95*, 65–87.
- (40) Wenzel, R. N. Resistance of solid surfaces to wetting by water. *Ind. Eng. Chem.* **1936**, *28*, 988–994.
- (41) Cassie, A.; Baxter, S. Wettability of porous surfaces. *Trans. Faraday Soc.* **1944**, *40*, 546–551.
- (42) Huhtamäki, T.; Tian, X.; Korhonen, J. T.; Ras, R. H. Surface-wetting characterization using contact-angle measurements. *Nat. Protoc.* **2018**, *13*, 1521–1538.
- (43) Kathel, P.; Mohanty, K. Wettability alteration in a tight oil reservoir. *Energy Fuels* **2013**, *27*, 6460–6468.
- (44) Zhao, G.; Yao, Y.; Adenutsi, C. D.; Feng, X.; Wang, L.; Wu, W. Transport behavior of oil in mixed wettability shale nanopores. *ACS Omega* **2020**, *5*, 31831–31844.
- (45) Wang, J.; Song, L.; Liu, Y.; Zhao, W.; Zhao, J.; Liu, B. Experimental Investigation of the Basic Characteristics and Wettability of Oil Shale Dust. *ACS Omega* **2021**, *6*, 14788–14795.
- (46) Saputra, I. W. R.; Adebisi, O.; Ladan, E. B.; Bagareddy, A.; Sarmah, A.; Schechter, D. S. The influence of oil composition, rock mineralogy, aging time, and brine pre-soak on shale wettability. *ACS Omega* **2021**, *7*, 85–100.
- (47) Ahmad, N.; Mateen, J.; Shehzad, K.; Mehmood, N.; Arif, F. *Shale Gas Potential of Lower Cretaceous Sembar Formation in Middle and Lower Indus Basin*; Pakistan, 2013.
- (48) Abro, W. A.; Shar, A. M.; Lee, K. S.; Narejo, A. A. An integrated analysis of mineralogical and microstructural characteristics and petrophysical properties of carbonate rocks in the lower Indus Basin, Pakistan. *Open Geosci.* **2019**, *11*, 1151–1167.
- (49) Shar, A. M.; Mahesar, A. A.; Abbasi, G. R.; Narejo, A. A.; Hakro, A. A. D. Influence of diagenetic features on petrophysical properties of fine-grained rocks of Oligocene strata in the Lower Indus Basin, Pakistan. *Open Geosci.* **2021**, *13*, 517–531.
- (50) Kadri, I. *Petroleum Geology of Pakistan*; Pakistan Petroleum Limited Karachi: Pakistan, 1995.
- (51) Iqbal, M. A.; Shah, S. I. *A Guide to the Stratigraphy of Pakistan*; Geological Survey of Pakistan, 1980.
- (52) Ali, M.; Sahito, M. F.; Jha, N. K.; Arain, S.; Memon, A.; Keshavarz, S.; Iglauer, A.; Saeedi, M.; Sarmadivaleh, M. Effect of nanofluid on CO<sub>2</sub>-wettability reversal of sandstone formation; implications for CO<sub>2</sub> geo-storage. *J. Colloid Interface Sci.* **2020**, *559*, 304–312.
- (53) Ali, M.; Yekeen, N.; Ali, M.; Hosseini, M.; Pal, N.; Keshavarz, A.; Iglauer, S.; Hoteit, H. Effects of Various Solvents on Adsorption of Organics for Porous and Nonporous Quartz/CO<sub>2</sub>: Implications for CO<sub>2</sub> Geo-Storage. *Energy Fuels* **2022**, *36*, 11089.
- (54) Krainer, S.; Hirn, U. Contact angle measurement on porous substrates: Effect of liquid absorption and drop size. *Colloids Surf., A* **2021**, *619*, 126503.
- (55) Mugele, F.; Bera, B.; Cavalli, A.; Siretanu, I.; Maestro, A.; Duits, M.; Cohen-Stuart, M.; van den Ende, D.; Stocker, I.; Collins, I. Ion adsorption-induced wetting transition in oil-water-mineral systems. *Sci. Rep.* **2015**, *5*, 1–8.
- (56) Saraji, S.; Goual, L.; Piri, M. Dynamic adsorption of asphaltenes on quartz and calcite packs in the presence of brine films. *Colloids Surf., A* **2013**, *434*, 260–267.
- (57) Mugele, F.; Siretanu, I.; Kumar, N.; Bera, B.; Wang, L.; de Ruiter, R.; Maestro, A.; Duits, M.; van den Ende, D.; Collins, I. Insights from ion adsorption and contact-angle alteration at mineral surfaces for low-salinity waterflooding. *SPE J.* **2016**, *21*, 1204–1213.
- (58) Arif, M.; Al-Yaseri, A. Z.; Barifcani, A.; Lebedev, M.; Iglauer, S. angles and CO<sub>2</sub>-brine interfacial tension: Implications for carbon geo-sequestration. *J. Colloid Interface Sci.* **2016**, *462*, 208–215.
- (59) Al-Yaseri, A.; Sarmadivaleh, M.; Saeedi, A.; Lebedev, M.; Barifcani, A.; Iglauer, S. N<sub>2</sub>+ CO<sub>2</sub>+ NaCl brine interfacial tensions and contact angles on quartz at CO<sub>2</sub> storage site conditions in the Gippsland basin, Victoria/Australia. *J. Petrol. Sci. Eng.* **2015**, *129*, 58–62.
- (60) Mirchi, V.; Saraji, S.; Goual, L.; Piri, M. Dynamic interfacial tension and wettability of shale in the presence of surfactants at reservoir conditions. *Fuel* **2015**, *148*, 127–138.
- (61) Sharifigaliuk, H.; Mahmood, S. M.; Padmanabhan, E. Evaluation of the wettability variation of shales by drop shape analysis approach. *SPE/AAPG/SEG Asia Pacific Unconventional Resources Technology Conference*; OnePetro, 2019.
- (62) Yang, D.; Gu, Y.; Tontiwachwuthikul, P. Wettability determination of the reservoir brine-rock system with dissolution of CO<sub>2</sub> at high pressures and elevated temperatures. *Energy Fuels* **2008**, *22*, 504–509.
- (63) Farokhpoor, R.; Bjørkvik, B. J.; Lindeberg, E.; Torsæter, O. Wettability behaviour of CO<sub>2</sub> at storage conditions. *Int. J. Greenh. Gas Control* **2013**, *12*, 18–25.
- (64) Sarmadivaleh, M.; Al-Yaseri, A. Z.; Iglauer, S. Influence of temperature and pressure on quartz-water-CO<sub>2</sub> contact angle and CO<sub>2</sub>-water interfacial tension. *J. Colloid Interface Sci.* **2015**, *441*, 59–64.
- (65) Al-Yaseri, A. Z.; Lebedev, M.; Barifcani, A.; Iglauer, S. Receding and advancing (CO<sub>2</sub>+ brine+ quartz) contact angles as a function of pressure, temperature, surface roughness, salt type and salinity. *J. Chem. Therm.* **2016**, *93*, 416–423.
- (66) De Ruijter, M.; Kölsch, P.; Voué, M.; De Coninck, J.; Rabe, J. Effect of temperature on the dynamic contact angle. *Colloids Surf., A* **1998**, *144*, 235–243.
- (67) Saraji, S.; Piri, M.; Goual, L. The effects of SO<sub>2</sub> contamination, brine salinity, pressure, and temperature on dynamic contact angles and interfacial tension of supercritical CO<sub>2</sub>/brine/quartz systems. *Int. J. Greenh. Gas Control* **2014**, *28*, 147–155.
- (68) Yekeen, N.; Padmanabhan, E.; Sevoo, A.; Kanesen, L.; Okunade, A.; Kanesen, L.; Okunade, O. A. Wettability of rock/CO<sub>2</sub>/brine systems: A critical review of influencing parameters and recent advances. *J. Ind. Eng. Chem.* **2020**, *88*, 1–28.
- (69) Najafi-Marghmaleki, A.; Barati-Harooni, A.; Soleymanzadeh, A.; Samadi, S. J.; Roshani, B.; Yari, A. Experimental investigation of effect of temperature and pressure on contact angle of four Iranian carbonate oil reservoirs. *J. Petrol. Sci. Eng.* **2016**, *142*, 77–84.
- (70) Hosseini, M.; Ali, M.; Fahimpour, J.; Keshavarz, A.; Iglauer, S. Assessment of rock-hydrogen and rock-water interfacial tension in shale, evaporite and basaltic rocks. *J. Nat. Gas Sci. Eng.* **2022**, *106*, 104743.
- (71) Pan, B.; Li, Y.; Zhang, M.; Wang, X.; Iglauer, S. Effect of total organic carbon (TOC) content on shale wettability at high pressure and high temperature conditions. *J. Petrol. Sci. Eng.* **2020**, *193*, 107374.
- (72) Chen, C.; Wan, J.; Li, W.; Song, Y. Water contact angles on quartz surfaces under supercritical CO<sub>2</sub> sequestration conditions: Experimental and molecular dynamics simulation studies. *Int. J. Greenh. Gas Control* **2015**, *42*, 655–665.
- (73) Akob, D. M.; Cozzarelli, I. M.; Dunlap, D. S.; Rowan, E. L.; Lorah, M. M. Organic and inorganic composition and microbiology of produced waters from Pennsylvania shale gas wells. *Appl. Geochem.* **2015**, *60*, 116–125.
- (74) Arif, M.; Lebedev, M.; Barifcani, A.; Iglauer, S. CO<sub>2</sub> storage in carbonates: Wettability of calcite. *Int. J. Greenh. Gas Control* **2017**, *62*, 113–121.
- (75) Lundegard, P. D.; Kharaka, Y. K. Distribution and occurrence of organic acids in subsurface waters. *Organic Acids in Geological Processes*; Springer, 1994, pp 40–69.
- (76) Pan, B.; Yin, X.; Iglauer, S. Rock-fluid interfacial tension at subsurface conditions: Implications for H<sub>2</sub>, CO<sub>2</sub> and natural gas geo-storage. *Int. J. Hydrogen Energy* **2021**, *46*, 25578–25585.

(77) Papp, E. A.; Csiha, C. Contact angle as function of surface roughness of different wood species. *Surface. Interfac.* **2017**, *8*, 54–59.